Unimolecular Rearrangements Connecting Hydroxyethylidene (CH_3-C-OH), Acetaldehyde (CH_3-CH=O), and Vinyl Alcohol (CH_2=CH-OH)

Brian J. Smith, Minh Tho Nguyen,[1a] Willem J. Bouma,[1b] and Leo Radom*

Contribution from the Research School of Chemistry, Australian National University, Canberra, A.C.T. 2601, Australia. *Received January 28, 1991*

Abstract: Ab initio molecular orbital theory at uniform and high levels has been used to study hydroxyethylidene and its isomers acetaldehyde and vinyl alcohol. Vinyl alcohol and hydroxyethylidene are predicted to lie 47 and 213 kJ mol^{-1}, respectively, above acetaldehyde. Hydroxyethylidene, despite its high relative energy, is predicted to be separated by significant barriers (118 and 98 kJ mol^{-1}, respectively) from its lower energy isomers acetaldehyde and vinyl alcohol. The transition structure for rearrangement of vinyl alcohol to acetaldehyde is found to lie lower in energy than the transition structures connecting hydroxyethylidene to acetaldehyde or vinyl alcohol. The rate-determining step for the production of CO from any of the three isomers is predicted to correspond to methane elimination from acetaldehyde, and this is consistent with observed effects.

There has been considerable recent experimental interest in the relative magnitudes of the barriers to intramolecular rearrangements connecting acetaldehyde (CH_3—CH=O, **1**), vinyl alcohol (CH_2=CH—OH, **2**), and hydroxyethylidene (CH_3—C—OH, **3**), but agreement as to the ordering of the barriers has yet to be reached.

Initial information on this point came from studies of the thermal decarboxylation of pyruvic acid for which it had been postulated that CH_3-C-OH (**3**) is a reaction intermediate.[2] Rosenfeld and Weiner[2] showed, through isotopic labeling experiments, that the formation of CH_3—CH=O (**1**) as the final product, does not involve the intermediacy of CH_2=CH—OH (**2**). They concluded that, if indeed CH_3-C-OH (**3**) is formed in the pyrolysis of pyruvic acid, the barrier for its rearrangement to **2** must be at least 14 kJ mol^{-1} greater than the barrier for rearrangement to **1**.

Subsequent kinetic studies by Yamamoto and Back[3] of the thermal decomposition of pyruvic acid yielded an activation energy of 116 kJ mol^{-1} for the decomposition. They concluded that this value was too low to permit access to CH_3-C-OH (**3**) as an intermediate, and thus questioned the interpretation of the earlier experiments.[2] More recently, Taylor[4] carried out a further study of the kinetics of the thermal decomposition of pyruvic acid. His data yielded an excellent linear Arrhenius plot, "completely typical of a unimolecular four-center reaction", and a significantly higher activation energy (173 kJ mol^{-1}) than that of Yamamoto and Back[3] for the decomposition.

In another recent experimental study, Wesdemiotis and McLafferty[5] used the technique of neutralization-reionization mass spectrometry (NRMS)[6] to study CH_3-C-OH. On the basis of labeling studies, these authors proposed that (i) the energy barrier required for the 1,2-hydrogen shift separating CH_3—C—OH (**3**) from CH_3—CH=O (**1**) should be smaller than the 1,2-hydrogen shift separating CH_3—C—OH (**3**) from CH_2=C-H—OH (**2**), and (ii) the transition structures associated with both these 1,2-hydrogen shifts should lie lower in energy than that associated with the 1,3-hydrogen shift that directly converts CH_2=CH—OH (**2**) to CH_3—CH=O (**1**).

There have been a number of previous ab initio studies of various aspects of the potential energy surface connecting **1**, **2**, and **3**.[7] These predicted, among other things, that the transition structure linking CH_3—C—OH (**3**) with CH_3—CH=O (**1**) (1,2-hydrogen shift) might lie up to 100 kJ mol^{-1} above that separating CH_2=CH—OH (**2**) from CH_3—CH=O (**1**) (1,3-hydrogen shift), in apparent conflict with some of the conclusions from the experimental studies.[2,5] Unfortunately, none of the previous theoretical studies examined all three relevant rearrangement processes, making reliable comparisons of the barrier heights somewhat difficult.

In order to obtain a consistent description of the energy surface and in an attempt to resolve the existing conflicting conclusions, we have carried out ab initio molecular orbital calculations at uniform and high levels of theory on the three isomers of interest, acetaldehyde (**1**), vinyl alcohol (**2**), and hydroxyethylidene (**3**), the three transition structures for unimolecular rearrangements connecting **1**, **2**, and **3**, and of various possible fragmentation processes.

Method and Results

Standard ab initio molecular orbital calculations[8] were carried out with modified versions[9] of the GAUSSIAN 82,[10] GAUSSIAN 86,[11] and GAUSSIAN 88[12] programs. Optimized geometries were obtained

(1) (a) Present address: Department of Chemistry, University of Leuven, Celestijnenlaan 200-F, B-3001-Leuven-Heverlee, Belgium. (b) Present address: CSIRO Division of Atmospheric Research, Aspendale, Victoria, Australia.

(2) (a) Rosenfeld, R. N.; Weiner, B. *J. Am. Chem. Soc.* **1983**, *105*, 3485. (b) Weiner, B. R.; Rosenfeld, R. N. *J. Org. Chem.* **1983**, *48*, 5362 and references therein.

(3) Yamamoto, S.; Back, R. A. *Can. J. Chem.* **1985**, *63*, 549.

(4) Taylor, R. *Int. J. Chem. Kinet.* **1987**, *19*, 709.

(5) Wesdemiotis, C.; McLafferty, F. W. *J. Am. Chem. Soc.* **1987**, *109*, 4760.

(6) For recent reviews, see: (a) Wesdemiotis, C.; McLafferty, F. W. *Chem. Rev.* **1987**, *87*, 485. (b) Terlouw, J. K.; Schwartz, H. *Angew. Chem., Int. Ed. Engl.* **1987**, *26*, 805. (c) Holmes, J. L. *Mass Spectrom. Rev.* **1989**, *8*, 513. (d) McLafferty, F. W. *Science* **1990**, *247*, 925.

(7) (a) Bouma, W. J.; Poppinger, D.; Radom, L. *J. Am. Chem. Soc.* **1977**, *99*, 6443. (b) Bouma, W. J.; Vincent, M. A.; Radom, L. *Int. J. Quantum Chem.* **1978**, *14*, 767. (c) Rodwell, W. R.; Bouma, W. J.; Radom, L. *Int. J. Quantum Chem.* **1980**, *18*, 107. (d) Faustov, V. I.; Yupit, S. S. *Russ. J. Phys. Chem. (Engl. Transl.)* **1982**, *56*, 1359. (e) Leska, J.; Zakova, M. *Collect. Czech. Chem. Commun.* **1982**, *47*, 1897. (f) Poirier, R. A.; Majlessi, D.; Zielinski, T. J. *J. Comput. Chem.* **1986**, *7*, 464. (g) Yadav, J. S.; Goddard, J. D. *J. Chem. Phys.* **1986**, *85*, 3975. (h) Goddard, J. D. *J. Mol. Struct.: THEOCHEM* **1987**, *149*, 39. (i) Murto, J.; Raaska, T.; Kunttu, H.; Rasanen, M. *J. Mol. Struct.: THEOCHEM* **1989**, *200*, 93. (j) Rasanen, M.; Raaska, T.; Kunttu, H.; Murto, J. *J. Mol. Struct.: THEOCHEM* **1990**, *208*, 79.

(8) Hehre, W. J.; Radom, L.; Schleyer, P. v. R.; Pople, J. A. *Ab Initio Molecular Orbital Theory*; John Wiley: New York, 1986.

(9) (a) Baker, J.; Nobes, R. H.; Poppinger, D.; Wong, M. W. Unpublished work. (b) Nobes, R. H.; Smith, B. J.; Riggs, N. V.; Wong, M. W. Unpublished work. (c) Baker, J. *J. Comput. Chem.* **1986**, *7*, 385. (d) Baker, J. *J. Comput. Chem.* **1987**, *8*, 563.

(10) Binkley, J. S.; Frisch, M. J.; DeFrees, D. J.; Raghavachari, K.; Whiteside, R. A.; Schlegel, H. B.; Fleuder, E. M.; Pople, J. A. GAUSSIAN 82; Carnegie-Mellon University: Pittsburgh, PA.

(11) Frisch, M. J.; Binkley, J. S.; Schlegel, H. B.; Raghavachari, K.; Melius, C. F.; Martin, R. L.; Stewart, J. J. P.; Bobrowicz, F. W.; Rohlfing, C. M.; Kahn, L. R.; DeFrees, D. J.; Seeger, R.; Whiteside, R. A.; Fox, D. J.; Fleuder, E. M.; Pople, J. A. GAUSSIAN 86; Carnegie-Mellon Quantum Chemistry Publishing Unit: Pittsburgh, PA, 1984.

0002-7863/91/1513-6452$02.50/0

at the Hartree–Fock (HF) level with the 6-31G(d) and 6-31G(d,p) basis sets and at the correlated level by using second-order Møller–Plesset perturbation theory (MP2) with the 6-31G(d) basis set. Harmonic vibrational frequencies were calculated at the HF/6-31G(d) level in order to characterize stationary points as minima or first-order saddle points and to estimate zero-point vibrational energies. Improved relative energies were obtained through calculations with larger basis sets, namely 6-311G(d,p), 6-311+G(d,p) and 6-311G(2df,p), and with more complete incorporation of electron correlation, namely MP3, MP4, and quadratic configuration interaction with single, double, and triple excitations (QCISD(T)).[13] Our most reliable results were obtained at the G1 level of theory.[14] This corresponds broadly to calculations at the QCISD(T)/6-311+G(2df,p) level, incorporating both isogyric and zero-point vibrational corrections. Unless otherwise noted, these are the values referred to in the text.

Optimized structural parameters at the HF/6-31G(d), HF/6-31G(d,p) and MP2/6-31G(d) levels for the equilibrium structures **1–3** and the transition structures **4–9**, shown in Figure 1, are listed in Table I. Corresponding total energies and relative energies for structures **1–6** at the various levels of theory are presented in Tables II and III, respectively. Table IV gives total energies at the G1 level of theory for a selection of possible dissociation fragments. Corresponding relative energies for the dissociation fragments are compared with experimental values in Table V. Energy data for transition structures (**7–9**) for methane and hydrogen elimination reactions are presented in Table VI. Schematic potential energy profiles for the rearrangement and dissociative processes involving the C_2H_4O isomers **1–3** are displayed in Figures 2 and 3.

Discussion

Equilibrium Structures. Our calculated structures (Table I) show the expected improvements compared with previously reported lower level results.[7] For acetaldehyde (**1**) and vinyl alcohol (**2**), for which experimental information is available,[15] our calculated MP2/6-31G(d) structural parameters (Table I) are very close to the experimental values.

We find that structures calculated at the HF/6-31G(d) and HF/6-31G(d,p) levels are very similar. The largest changes occur for bridging C–H and O–H bond lengths, but even in these cases the differences are small. More significant structural changes are noticeable at the MP2/6-31G(d) level, with a characteristic lengthening of bonds. As we shall see below, however, the effect of such structural differences (i.e. MP2/6-31G(d) or HF/6-31G(d,p) compared with HF/6-31G(d)) on calculated relative energies is very small.

We turn now to a consideration of relative energies (Table III) and examine first the energy difference between acetaldehyde (**1**) and vinyl alcohol (**2**). This energy difference is of importance since acetaldehyde and vinyl alcohol represent the prototypical keto–enol pair. The results appear to be surprisingly sensitive to the inclusion in the basis set of p functions on hydrogen, with a 14 kJ mol^{-1} change in going from HF/6-31G(d) to HF/6-31G(d,p). Our calculations also indicate that the energy difference between **2** and **1** decreases consistently as the size of the basis set increases. However, calculations at the MP2 level show no further change in going from the 6-311+G(2df,p) to the 6-311+G(3df,2p) basis set.[16] Our best calculated relative energy of 47 kJ mol^{-1} (in favor of acetaldehyde) is in good agreement with the experimental value[17] of 41 ± 8 kJ mol^{-1}.

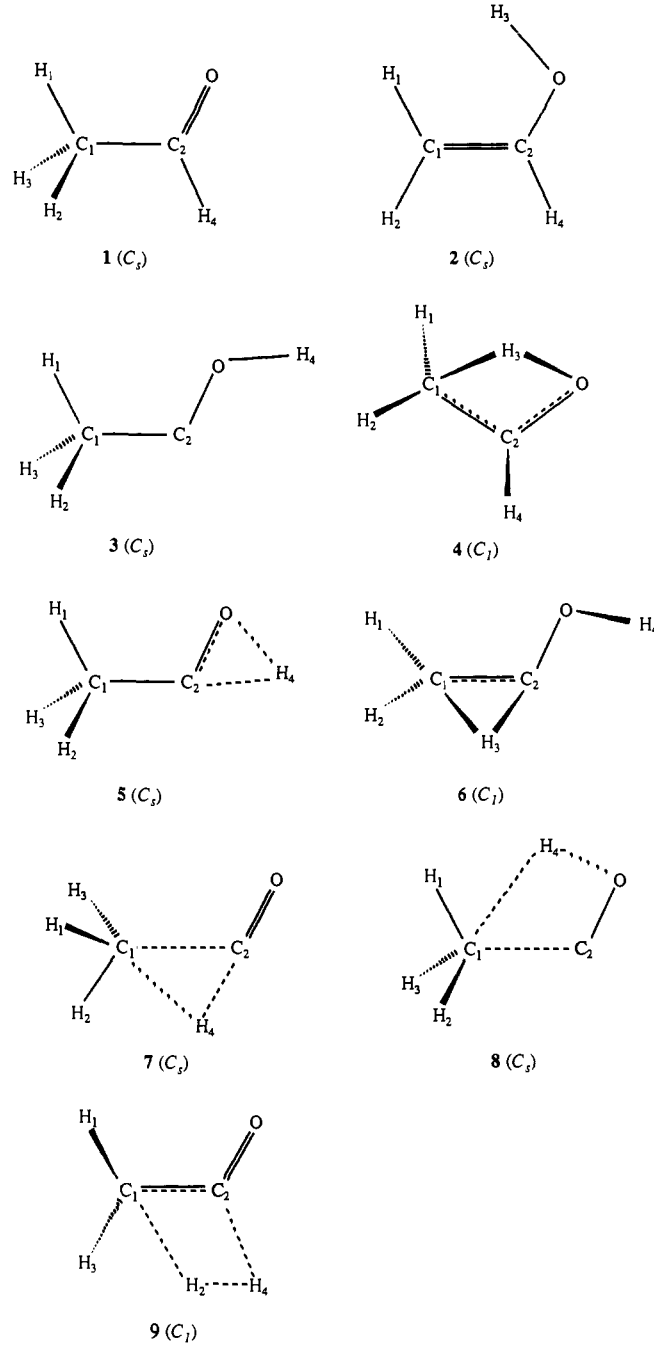

Figure 1. C_2H_4O equilibrium structures (**1–3**) and transition structures (**4–9**).

Two previous estimates of the energy difference between hydroxyethylidene (**3**) and acetaldehyde (**1**) have been reported. Rosenfeld and Weiner[2a] estimated a value of 251 kJ mol^{-1} on the basis of an ab initio energy difference between H_2CO and HCOH and the use of Benson additivity terms. More recently, Yadav and Goddard[7g] proposed a value of 259 kJ mol^{-1}, assuming additivity of CISD/3-21G and HF/6-31G(d) results. Our best estimate, at a substantially higher level of theory, is the lower value of 213 kJ mol^{-1}.

An assessment of the reliability of this value is provided by a consideration of the situation for the lower homologous pair, formaldehyde/hydroxymethylene, for which an experimental estimate of the energy difference is available from an ion-cyclotron-resonance experiment.[18] The energy difference between the

(12) Frisch, M. J.; Head-Gordon, M.; Schlegel, H. B.; Raghavachari, K.; Binkley, J. S.; Gonzalez, C.; DeFrees, D. J.; Fox, D. J.; Whiteside, R. A.; Seeger, R.; Melius, C. F.; Baker, J.; Kahn, L. R.; Stewart, J. J. P.; Fleuder, E. M.; Topiol, S.; Pople, J. A. GAUSSIAN 88, Gaussian Inc.: Pittsburgh, PA, 1988.

(13) Pople, J. A.; Head-Gordon, M.; Raghavachari, K. *J. Chem. Phys.* **1987**, *87*, 5968.

(14) Pople, J. A.; Head-Gordon, M.; Fox, D. J.; Raghavachari, K.; Curtiss, L. A. *J. Chem. Phys.* **1989**, *90*, 5622.

(15) (a) Kilb, R. W.; Lin, C. C.; Wilson, E. B. *J. Chem. Phys.* **1957**, *26*, 1695. (b) An experimental structure for vinyl alcohol (**2**) is given in: Smith, B. J.; Radom, L. *J. Am. Chem. Soc.* **1990**, *112*, 7525.

(16) Calculated total energies at MP2/6-311+G(2df,p) are −153.524 12 (CH_3CHO) and −153.506 83 (CH_2CHOH) hartree, and at MP2/6-311+G(3df,2p) are −153.538 01 (CH_3CHO) and −153.520 89 (CH_2CHOH) hartree.

(17) Holmes, J. H.; Lossing, F. P. *J. Am. Chem. Soc.* **1982**, *104*, 2648.

Table I. Optimized Equilibrium Structures (1–3) and Transition Structures (4–9)

parameter	HF/ 6-31G(d)	HF/ 6-31G(d,p)	MP2/ 6-31G(d)	exptl	parameter	HF/ 6-31G(d)	HF/ 6-31G(d,p)	MP2/ 6-31G(d)	exptl
				acetaldehyde (1)					
C_1–C_2	1.504	1.503	1.501	1.501[a]	$<C_1C_2O$	124.4	124.4	124.4	123.9
C_2–O	1.188	1.188	1.222	1.216	$<C_2C_1H_1$	110.3	110.3	109.9	110.6
C_1–H_1	1.082	1.082	1.090	1.086	$<C_2C_1H_{23}$	124.8	124.7	124.9	126.9
C_1–H_2	1.087	1.087	1.095	1.086	$<H_2C_1H_3$	107.2	107.2	107.2	108.3
C_2–H_4	1.095	1.097	1.109	1.114	$<C_1C_2H_4$	115.3	115.3	115.3	117.5
				vinyl alcohol (2)					
C_1–C_2	1.318	1.318	1.336	1.335[b]	$<C_1C_2O$	126.9	126.9	126.8	126.0
C_2–O	1.347	1.346	1.367	1.369	$<C_2C_1H_1$	122.4	122.3	122.3	121.5
C_1–H_1	1.077	1.077	1.086	1.084	$<C_2C_1H_2$	120.1	120.0	120.0	119.5
C_1–H_2	1.073	1.073	1.081	1.081	$<C_1C_2H_4$	122.4	122.2	122.9	123.5
C_2–H_4	1.073	1.075	1.085	1.080	$<C_2OH_3$	110.4	110.6	108.2	108.5
O–H_3	0.948	0.944	0.974	0.962					
				hydroxyethylidene (3)					
C_1–C_2	1.502	1.501	1.499		$<C_1C_2O$	107.9	107.9	106.3	
C_2–O	1.306	1.305	1.328		$<C_2C_1H_1$	114.8	114.7	115.0	
C_1–H_1	1.087	1.087	1.096		$<C_2C_1H_{23}$	120.7	120.5	120.0	
C_1–H_2	1.087	1.087	1.095		$<H_2C_1H_3$	106.0	105.9	105.8	
O–H_4	0.950	0.946	0.977		$<C_2OH_4$	109.1	109.2	106.9	
				TS:2 → 1 (4)					
C_1–C_2	1.421	1.421	1.405		$<C_1C_2O$	109.2	109.0	111.0	
C_2–O	1.252	1.251	1.294		$<C_2C_1H_1$	110.0	110.0	112.9	
C_1–H_1	1.085	1.084	1.091		$<C_2C_1H_2$	120.7	120.7	121.7	
C_1–H_2	1.079	1.078	1.086		$<C_1C_2H_4$	131.6	131.6	130.6	
C_1–H_3	1.518	1.502	1.520		$<C_2C_1H_3$[c]	65.6	65.3	66.4	
C_2–H_4	1.081	1.082	1.092		$<H_1C_1C_2O$	73.8	73.8	65.3	
O–H_3	1.234	1.228	1.293		$<H_2C_1C_2O$	−152.4	−151.9	−153.6	
					$<H_4C_2C_1O$	177.2	177.0	178.1	
					$<H_3C_1C_2O$	−7.9	−8.2	−9.8	
				TS:3 → 1 (5)					
C_1–C_2	1.491	1.491	1.490		$<C_1C_2O$	118.0	118.1	115.1	
C_2–O	1.275	1.275	1.325		$<C_2C_1H_1$	110.3	110.3	110.4	
C_1–H_1	1.087	1.087	1.096		$<C_2C_1H_{23}$	123.9	123.8	123.6	
C_1–H_2	1.086	1.086	1.094		$<H_2C_1H_3$	107.1	107.1	107.0	
C_2–H_4	1.224	1.215	1.285		$<C_2OH_4$	59.9	59.4	61.9	
O–H_4	1.171	1.169	1.158						
				TS:3 → 2 (6)					
C_1–C_2	1.368	1.369	1.391		$<C_1C_2O$	112.2	112.4	110.7	
C_2–O	1.358	1.357	1.370		$<C_2C_1H_1$	124.1	124.1	123.9	
C_1–H_1	1.084	1.084	1.095		$<C_2C_1H_2$	118.4	118.2	117.8	
C_1–H_2	1.075	1.076	1.085		$<C_2C_1H_3$[c]	52.9	52.9	55.0	
C_1–H_3	1.415	1.412	1.355		$<C_2OH_4$	108.1	108.2	106.1	
C_2–H_3	1.240	1.240	1.268		$<H_1C_1C_2O$	4.2	4.1	4.1	
O–H_4	0.945	0.941	0.970		$<H_2C_1C_2O$	179.7	179.3	175.8	
					$<H_3C_1C_2O$	−109.0	−109.4	−109.3	
					$<H_4OC_2C_1$	178.1	177.9	174.4	
				TS:1 → CH_4 + CO (7)					
C_1–C_2	2.067	2.050	2.076		$<C_1C_2O$	110.0	110.4	108.0	
C_2–O	1.146	1.147	1.186		$<C_1C_2H_4$[c]	53.4	53.3	55.9	
C_1–H_1	1.084	1.084	1.091		$<C_2C_1H_2$	123.8	123.2	123.9	
C_1–H_2	1.088	1.089	1.095		$<C_2C_1H_{13}$	108.6	109.3	104.9	
C_1–H_4	1.666	1.649	1.721		$<H_1C_1H_3$	110.8	110.8	111.8	
C_2–H_4	1.097	1.095	1.093						
				TS:3 → CH_4 + CO (8)					
C_1–C_2	1.887	1.877	1.803		$<C_1C_2O$	101.0	101.0	103.7	
C_2–O	1.234	1.234	1.287		$<C_2OH_4$	72.4	71.4	67.6	
C_1–H_1	1.102	1.102	1.113		$<C_2C_1H_1$	127.8	126.2	126.9	
C_1–H_2	1.082	1.082	1.089		$<C_2C_1H_{23}$	110.2	111.3	110.4	
C_1–H_4	1.442	1.423	1.401		$<H_2C_1H_3$	110.7	111.0	111.5	
O–H_4	1.171	1.174	1.214						
				TS:1 → CH_2CO + H_2 (9)					
C_1–C_2	1.374	1.372	1.401		$<C_1C_2O$	141.9	142.1	141.4	
C_2–O	1.186	1.187	1.205		$<C_2C_1H_1$	120.8	120.8	120.2	
C_1–H_1	1.077	1.077	1.088		$<C_2C_1H_2$	53.9	53.5	57.6	
C_1–H_2	1.652	1.631	1.629		$<C_2C_1H_3$	118.2	118.1	115.8	
C_1–H_3	1.072	1.073	1.085		$<C_1C_2H_4$	101.2	101.3	99.6	
C_2–H_4	1.300	1.304	1.343		$<OC_2C_1H_1$	10.8	9.5	13.6	
H_2–H_4	1.000	0.998	1.013		$<OC_2C_1H_2$	−131.4	−131.8	−130.0	
					$<OC_2C_1H_3$	172.6	172.4	167.0	
					$<OC_2C_1H_4$	−165.0	−165.4	−159.1	

[a] From ref 14. [b] From ref 15. [c] Nonindependent parameter.

Table II. Calculated Total Energies (hartrees) for Stationary Points on the C_2H_4O Potential Energy Surface[a]

	CH_3—CH=O (1)	CH_2=CH—OH (2)	CH_3—C—OH (3)	TS:1 → 2 (4)	TS:1 → 3 (5)	TS:2 → 3 (6)
HF/6-31G(d)//HF/6-31G(d)	−152.915 97	−152.888 89	−152.832 91	−152.770 82	−152.753 73	−152.771 19
HF/6-31G(d,p)//HF/6-31G(d,p)	−152.922 59	−152.901 00	−152.844 24	−152.783 11	−152.766 43	−152.785 55
MP2/6-31G(d)//MP2/6-31G(d)[b]	−153.358 97	−153.332 16	−153.262 43	−153.237 71	−153.215 61	−153.218 05
MP2/6-31G(d,p)//HF/6-31G(d)	−153.376 35	−153.354 39	−153.284 77	−153.258 03	−153.238 33	−153.244 16
MP2/6-31G(d,p)//HF/6-31G(d,p)	−153.376 38	−153.354 15	−153.284 57	−153.258 01	−153.238 44	−153.244 04
MP2/6-31G(d,p)//MP2/6-31G(d)	−153.378 42	−153.355 50	−153.285 75	−153.260 74	−153.239 67	−153.243 77
MP2/6-311G(d,p)//MP2/6-31G(d)	−153.442 43	−153.422 37	−153.355 07	−153.329 09	−153.308 10	−153.314 67
MP3/6-311G(d,p)//MP2/6-31G(d)	−153.457 02	−153.440 34	−153.376 95	−153.335 89	−153.316 55	−153.332 94
MP4/6-311G(d,p)//MP2/6-31G(d)	−153.487 68	−153.466 07	−153.403 63	−153.373 25	−153.355 80	−153.360 25
QCISD(T)/6-311G(d,p)//MP2/6-31G(d)	−153.485 89	−153.466 23	−153.404 60	−153.370 51	−153.352 91	−153.360 98
MP4/6-311+G(d,p)//MP2/6-31G(d)	−153.494 81	−153.474 01	−153.412 09	−153.380 94	−153.363 95	−153.370 05
MP4/6-311G(2df,p)//MP2/6-31G(d)	−153.566 99	−153.547 26	−153.481 09	−153.454 83	−153.434 81	−153.439 90
G1[c]	−153.574 07	−153.556 09	−153.492 77	−153.466 53	−153.447 83	−153.455 58

[a] Frozen-core results reported unless otherwise noted. [b] Full set of orbitals used in correlation treatment. [c] Scaled zero-point vibrational energies are 53.52 (**1**), 54.53 (**2**), 53.01 (**3**), 48.41 (**4**), 47.50 (**5**), and 50.11 (**6**) mhartree; higher level correction is −55.26 mhartree.

Table III. Calculated Relative Energies (kJ mol^{-1}) for Stationary Points on the C_2H_4O Potential Energy Surface[a]

	CH_3—CH=O (1)	CH_2=CH—OH (2)	CH_3—C—OH (3)	TS:1 → 2 (4)	TS:1 → 3 (5)	TS:2 → 3 (6)
HF/6-31G(d)//HF/6-31G(d)	0	71	218	381	462	380
HF/6-31G(d,p)//HF/6-31G(d,p)	0	57	206	366	410	360
MP2/6-31G(d)//MP2/6-31G(d)	0	70	253	318	376	370
MP2/6-31G(d,p)//HF/6-31G(d)	0	58	240	311	362	347
MP2/6-31G(d,p)//HF/6-31G(d,p)	0	58	241	311	362	347
MP2/6-31G(d,p)//MP2/6-31G(d)	0	60	243	309	364	354
MP2/6-311G(d,p)//MP2/6-31G(d)	0	53	229	298	353	335
MP3/6-311G(d,p)//MP2/6-31G(d)	0	44	210	318	369	326
MP4/6-311G(d,p)//MP2/6-31G(d)	0	57	221	300	346	335
QCISD(T)/6-311G(d,p)//MP2/6-31G(d)	0	52	213	303	349	328
MP4/6-311+G(d,p)//MP2/6-31G(d)	0	55	217	299	344	328
MP4/6-311G(2df,p)//MP2/6-31G(d)	0	52	226	294	347	334
G1	0	47	213	282	331	311

[a] Calculated from total energies in Table II.

Table IV. G1 Energies (E(G1), hartrees) and Experimental Heats of Formation ($\Delta H_f°_0$, kJ mol^{-1}) for Acetaldehyde (**1**) and C_2H_4O Dissociation Products

species	E(G1)[a]	$\Delta H_f°_0$[b]	species	E(G1)[a]	$\Delta H_f°_0$[b]
CH_3CHO	−153.574 07[c]	−155.0	$CH_2CH^•$	−77.738 48[f]	292.0[j]
$CH_3CO^•$	−152.932 79[d]	−16.5[e,f]	$OH^•$	−75.642 14	38.4
$CH_2CHO^•$	−152.921 86[g]	19.9[f,h]	CH_4	−40.407 72	−66.8
CH_2CO	−152.368 41[d]	−44.6	$CH_3^•$	−39.742 54	149.0
$HCO^•$	−113.697 46	44.4[f]	H_2	−1.165 01	0
CO	−113.177 22	−113.8	$H^•$	−0.500 00	216.0

[a] Taken from ref 14 unless otherwise noted. [b] Taken from ref 20 unless otherwise noted. [c] Present work. [d] Reference 27. [e] Reference 21. [f] Temperature correction to experimental $\Delta H_f°_{298}$ values to give $\Delta H_f°_0$ values obtained from calculated vibrational frequencies. [g] Reference 28. [h] Reference 22. [i] Reference 26. [j] Reference 23.

two H_2CO isomers, calculated at the G1 level,[19] is 220 kJ mol^{-1} and this agrees well with the experimental value of 227 ± 8 kJ mol^{-1}. This good agreement lends confidence to our predicted energy difference for the acetaldehyde/hydroxyethylidene pair.

Fragmentation Products. Calculated relative energies for various possible fragmentation products are compared with experimental values[20-24] in Table V. In general, the agreement between theory and experiment is satisfactory. Discrepancies greater than the target accuracy of 0.15 eV (15 kJ mol^{-1}) for G1 theory[14,25] are found for comparisons involving the vinyl radical and acetyl radical. In the case of the vinyl radical, it has been suggested[23,26] that the experimental[23] $\Delta H_f°_0$, calculated from the measured adiabatic ionization energy, may be too low by about 15 kJ mol^{-1} because of difficulties in observing the 0→0 transition, which in turn has been attributed to the markedly different structures of the vinyl radical (open) and vinyl cation (bridged). Such a correction would bring the theoretical and experimental relative energies in the present situation into good agreement. For dissociation to the acetyl radical, the discrepancy between theory

Table V. Comparison of Calculated (G1) and Experimental Relative Energies (kJ mol^{-1}) of C_2H_4O Dissociation Products[a]

species	theor	exptl
CH_3CHO	0	0
CH_4 + CO	−29	−26
CH_2CO + H_2	107	110
$CH_3^•$ + $HCO^•$	352	348
$CH_3CO^•$ + $H^•$	371	355
$CH_2CHO^•$ + $H^•$	400	391
$CH_3^•$ + CO + $H^•$	405	406
$CH_2CH^•$ + $OH^•$	508	485

[a] Calculated from energies in Table IV.

(18) Pan, C. F.; Hehre, W. J. *J. Phys. Chem.* **1982**, *86*, 1252.
(19) For CH_2O, E(G1) = −114.337 29 hartree (ref 14). Relevant results for HCOH are: E(MP4) = −114.177 82 hartree, Δ(+) = −6.92, Δ(2df) = −56.73, Δ(QCI) = −0.97, Δ(HLC) = −36.84, Δ(ZPVE) = 25.84 mhartree, leading to E(G1) = −114.253 44 hartree.
(20) Lias, S. G.; Bartmess, J. E.; Liebman, J. F.; Holmes, J. L.; Levin, R. D.; Mallard, W. G. *J. Phys. Chem. Ref. Data* **1988**, *17*, Suppl. 1.
(21) Nimlos, M. R.; Soderquist, J. A.; Ellison, G. B. *J. Am. Chem. Soc.* **1989**, *111*, 7675.
(22) Ellison, G. B.; Engelking, P. C.; Lineberger, W. C. *J. Phys. Chem.* **1982**, *86*, 4873.
(23) Berkowitz, J.; Mayhew, C. A.; Ruscic, B. *J. Chem. Phys.* **1988**, *88*, 7396.
(24) Relative energies are quoted at 0 K. Where $\Delta H_f°_0$ values are not available in the literature, these have been obtained by correcting the experimental $\Delta H_f°_{298}$ values with our calculated ab initio frequencies.
(25) Curtiss, L. A.; Jones, C.; Trucks, G. W.; Raghavachari, K.; Pople, J. A. *J. Chem. Phys.* **1990**, *93*, 2537.
(26) Curtiss, L. A.; Pople, J. A. *J. Chem. Phys.* **1988**, *88*, 7405.

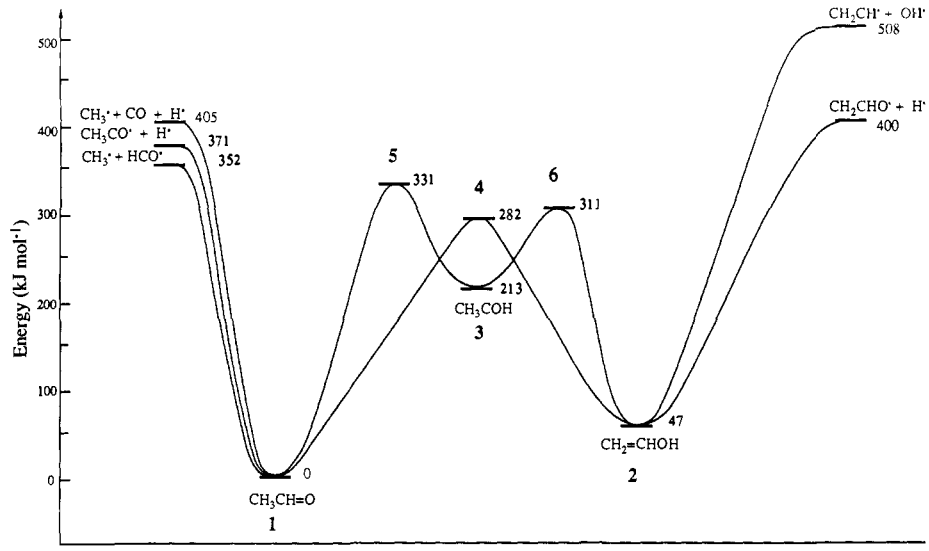

Figure 2. Schematic potential energy profile (G1 level) for unimolecular rearrangements among C_2H_4O isomers (1–3) and their simple fragmentation reactions.

and experimental energies is again just outside the target accuracy. On the basis of this and other results,[27,28] it would seem that the current experimental heat of formation for the acetyl radical[21] may be slightly too low.

Rearrangement Reactions. A schematic energy profile showing the rearrangement processes connecting the isomers **1**, **2**, and **3** and their dissociation reactions is shown in Figure 2. Calculated relative energies at a number of levels of theory are included in Table III. Our calculations are consistent with the experiment[5] in predicting that hydroxyethylidene (**3**), despite its very high energy (213 kJ mol^{-1} above **1**), should be observable. It is separated from the lower energy isomers acetaldehyde (**1**) and vinyl alcohol (**2**) by significant barriers (of 118 and 98 kJ mol^{-1}, respectively).

Our calculations are, however, not consistent with the ordering of energies of the transition structures **4**, **5**, and **6**, as deduced from the experiment. At all levels of theory that incorporate electron correlation (Table IV), we find the energy ordering **4** < **6** < **5**. This is precisely the reverse of the ordering proposed by Wesdemiotis and McLafferty,[5] and also is in conflict with the conclusion of Rosenfeld and Weiner[2] that **3** rearranges to **1** but not to **2**.

Our best values for the relative energies of transition structures **4**, **5**, and **6** are 282, 331, and 311 kJ mol^{-1}, respectively, compared with experimental estimates[5] for the latter two of approximately 314 and 335 kJ mol^{-1}, respectively. Thus, we predict that rearrangement of hydroxyethylidene (**3**) to vinyl alcohol (**2**) requires a smaller barrier (by 20 kJ mol^{-1}) than rearrangement to acetaldehyde (**1**). The transition structure **4** for rearrangement of vinyl alcohol (**2**) to acetaldehyde (**1**) lies a further 29 kJ mol^{-1} lower in energy.

In the light of the apparent conflict between theory and experiment, it is important to investigate possible sources of uncertainty in the theoretical results. Examination of Table III reveals the following points:

(i) The variation in relative energies associated with calculations (at the MP2/6-31G(d,p) level) at HF/6-31G(d), HF/6-31G(d,p), and MP2/6-31G(d) optimized geometries is very small, producing differences typically less than 3 kJ mol^{-1}. Thus, we believe it to be unlikely that reoptimization of geometries at still higher levels of theory will be important.

(ii) There is comparatively little variation among relative energies calculated at the various correlated levels: MP2, MP3, MP4, and QCISD(T). Most importantly, the ordering of the relative energies of the minima and transition structures does not change at any level of theory. This suggests that more precise treatments of electron correlation are unlikely to have a significant effect on relative energies and, in particular, are unlikely to affect the energy ordering.

(iii) The energies relative to that of **1** are found to change only slightly (≤7 kJ mol^{-1}) with inclusion of diffuse functions in the basis set or with the addition of a second set of d functions and an f function set. On this basis, we conclude that further basis set enhancement is also unlikely to change the ordering of the energies of transition structures **4**–**6**.

Thus, we find that an analysis of our present theoretical results gives no indication that a change in ordering of the energies of the rearrangement transition structures is likely to occur at higher levels of theory. The apparent discrepancy between theory and experiment[2,5] with respect to the energy ordering of **4**, **5**, and **6** remains. It is therefore desirable to reexamine the experimental results, and we make some preliminary brief comments here.

Scheme I

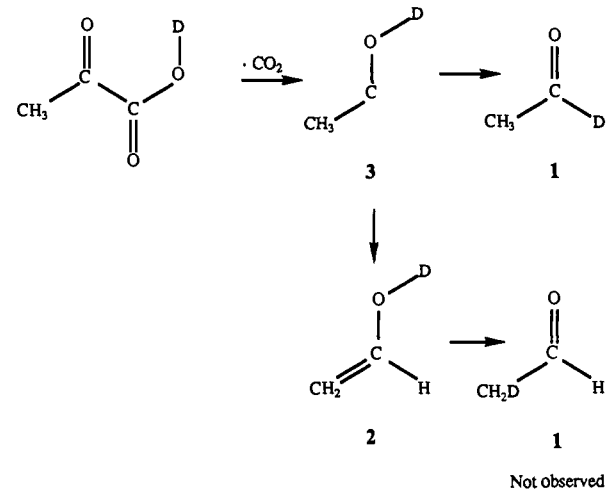

Scheme II

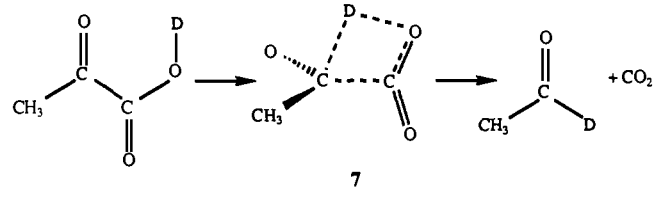

(27) Smith, B. J.; Radom, L. *Int. J. Mass Spectrom. Ion Processes* **1990**, *101*, 209.

(28) Smith, B. J.; Radom, L. Unpublished work.

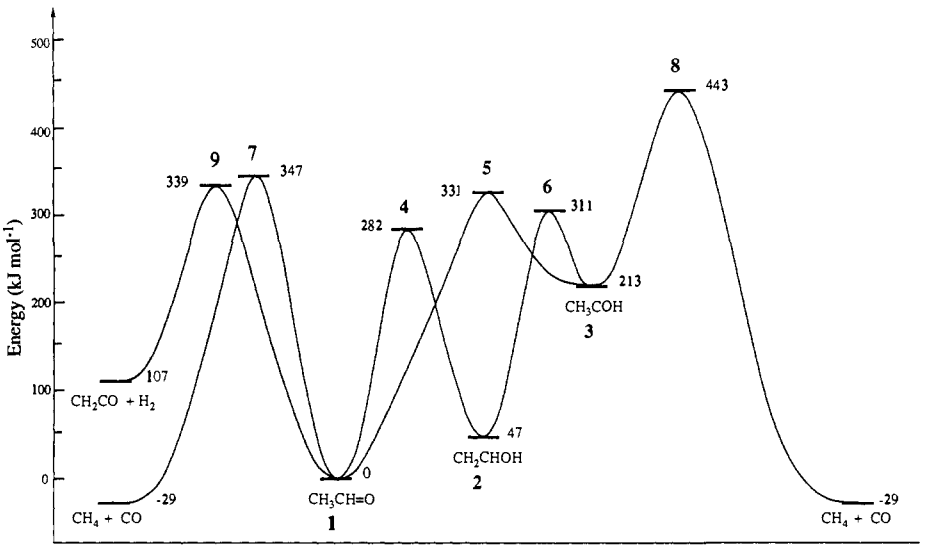

Figure 3. Schematic potential energy profile (G1 level) showing elimination reactions involving C_2H_4O isomers (**1**–**3**).

Table VI. G1 Energy Contributions from Transition Structures[a]

	MP4	Δ(+)	Δ(2df)	Δ(QCI)	Δ(HLC)	Δ(ZPVE)	E(G1)	ΔE^b
TS:$CH_3CHO \rightarrow CH_4 + CO$ **7**	−153.352 26	−5.89	−79.19	4.07	−55.26	46.84	−153.441 69	347
TS:$CH_3COH \rightarrow CH_4 + CO$ **8**	−153.314 27	−5.90	−77.64	3.14	−55.26	44.60	−153.405 33	443
TS:$CH_3CHO \rightarrow CH_2CO + H_2$ **9**	−153.349 94	−7.86	−82.02	4.98	−55.26	45.11	−153.444 99	339

[a] Units are hartrees for total energies and millihartrees for energy differences unless otherwise noted. [b] Energies relative to CH_3CHO (**1**) (kJ mol^{-1}).

For the thermal decomposition to pyruvic acid to produce acetaldehyde (**1**) + CO_2, two mechanisms have been proposed.[2-4] The preferred mechanism (Scheme I) involves hydroxyethylidene (**3**) as an intermediate. When O-*d*-labeled pyruvic acid is used as starting material, CH_2DCHO is not observed, which rules out the intermediacy of vinyl alcohol (**2**), and leads to the conclusion that rearrangement of **3** to **1** occurs more readily than to **2** (and hence that **5** lies lower in energy than **6**).

The alternative mechanism for the pyruvic acid decarboxylation[2-4] involves a direct intramolecular rearrangement with a four-membered cyclic transition structure (**7**) (Scheme II). If this is in fact the preferred reaction pathway,[3,4] the observation of CH_3CDO but not CH_2DCHO does not have any implications concerning rearrangement barriers involving **3**, and the apparent conflict with theory is removed. It is relevant to note, however, that recent calculations[29] probing the decarboxylation of the lower homologue, glyoxylic acid (HCOCOOH), showed that the transfer of the hydroxy hydrogen to the oxygen center in a process with $HOCHCO_2$ as an intermediate, which then produces hydroxymethylene, HCOH, and subsequently formaldehyde, H_2CO, is more favorable than transfer to the carbon, which generates formaldehyde directly. We are currently examining the energy requirements of these two competing mechanisms in pyruvic acid.

For the NRMS study,[5] the conclusions concerning the relative barrier heights for the rearrangement reactions are based largely on subtle differences between the various spectra, on which we cannot usefully comment. However, one of our results that may shed light on some of the experimental observations is the calculation of the mechanism and barrier for the production of carbon monoxide from acetaldehyde (**1**) (Figure 3). We predict that a single-step elimination of methane[30] (rather than stepwise loss of $CH_3^\bullet$ and $H^\bullet$) occurs via transition structure **7** with a barrier of 347 kJ mol^{-1}. This is the lowest energy pathway for production of CO from acetaldehyde, and the calculated exothermicity (29 kJ mol^{-1}) is very close to the experimental value (26 kJ mol^{-1}) (Table V). The fact that the energy of the transition structure **7** for methane elimination lies higher than the energies of transition structures **4**–**6** for interconversion of the three stable isomers **1**–**3** suggests that reaction via **7** represents the rate-determining step for the formation of the CO observed in the NRMS spectra of *any of the isomers* **1**–**3**.

The prediction of a rate-determining methane elimination reaction for **1**–**3** has important consequences with respect to the observation of significant isotope effects in NRMS experiments in which the neutrals are collisionally activated.[5] For example, the observation in such experiments of decreased formation of CO from CH_3CDO compared with CH_3CHO is consistent with this mechanism. Significantly, the observation[5] of a similar reduction in the production of CO from $CH_2{=}CD{-}OH$ but not for $CH_2{=}CH{-}OD$ is again consistent with this mechanism, indicating an initial non-rate-determining 1,3-hydrogen (or deuterium) shift giving $CH_3CD{=}O$ or $CH_2DCH{=}O$, respectively, followed by the rate-determining elimination of methane (Figure 3). Under this interpretation, the rearrangement of vinyl alcohol (**2**) to acetaldehyde (**1**) does indeed occur in the collisionally activated NRMS experiments,[5] removing part of the apparent discrepancy between theory and experiment.

We note that direct methane elimination from CH_3COH (**3**) is significantly more costly energetically than the process in which there is initial rearrangement of **3** to **1** followed by methane elimination from **1** via **7**. The energy of the transition structure **8** for the direct elimination process is 443 kJ mol^{-1} (relative to **1**) as opposed to 347 kJ mol^{-1} for **7**, the transition structure for the rearrangement–elimination reaction (Figure 3). The rearrangement of CH_3COH (**3**) to CH_3CHO (**1**) can take place either in a one-step process via transition structure **5** or in a two-step process via vinyl alcohol (**2**) and the transition structures **6** and **4**. The latter pathway has a slightly lower energy requirement (311 kJ mol^{-1}) than the former (331 kJ mol^{-1}). Intriguingly, the predicted isotope effect for methane elimination from CH_3COD depends on the pathway undertaken. Rearrangement of CH_3COD via **5** would produce CH_3CDO, which *would* show an isotope effect

(29) Bock, C. W.; Redington, R. L. *J. Phys. Chem.* **1988**, *92*, 1178.

(30) The elimination of CH_4 and H_2 from acetaldehyde has been investigated previously: (a) Yadav, J. S.; Goddard, J. D. *J. Chem. Phys.* **1986**, *84*, 2682. (b) Yu, H.; Goddard, J. D. To be published.

(31) **Note Added in Proof**: We find, at the G2 level (Curtiss, L. A.; Raghavachari, K.; Trucks, G. W.; Pople, J. A. *J. Chem. Phys.* **1991**, *94*, 7221), total energies for **1**–**6** of −153.576 82, −153,559 02, −153.495 92, −153.468 84, −153.451 05, and −153.458 75 hartree, respectively, and relative energies of 0, 47, 212, 283, 330, and 310 kJ mol^{-1}, respectively, very close to the G1 results.

for methane elimination, whereas rearrangement via **6**, **2**, and **4** would produce CH_2DCHO, which would *not*. It would be of interest to see whether experimental isotope effects support the lower energy two-step pathway or the higher energy one-step rearrangement of **3** to **1**.

Our calculations indicate that elimination of molecular hydrogen from acetaldehyde[30] via transition structure **9** has a marginally lower energy requirement (339 kJ mol^{-1}) than the methane elimination via **7** (347 kJ mol^{-1}).

Concluding Remarks

(i) We find that vinyl alcohol (**2**) lies 47 kJ mol^{-1} higher and hydroxyethylidene (**3**) 213 kJ mol^{-1} higher in energy than acetaldehyde.

(ii) Hydroxyethylidene (**3**), although a high-energy species, is predicted to be separated by significant barriers (118 and 98 kJ mol^{-1}, respectively) from its lower energy isomers **1** and **2**; it should thus be observable, consistent with experiment.

(iii) The energy ordering of the transition structures (**4**, **5**, and **6**, respectively) for the rearrangements **1** → **2**, **1** → **3**, and **2** → **3** is **4** < **6** < **5**. This is in apparent conflict with conclusions based on experimental observations.

(iv) The rate-determining step for the production of CO from any of the three isomers **1**-**3** is predicted to correspond to the elimination of methane from acetaldehyde (**1**) (preceded in the case of both **2** and **3** by lower energy rearrangements to **1**), and this is consistent with isotope effects observed in NRMS studies.

Acknowledgment. We thank Professor Fred McLafferty for helpful discussions, Professor J. D. Goddard for providing us with results prior to publication, and gratefully acknowledge a generous allocation of time on the Fujitsu FACOM VP-100 of the Australian National University Supercomputer Facility.

Supplementary Material Available: Calculated (HF/6-31G(d)) vibrational frequencies for structures **1**-**9** (Table VII) (1 page). Ordering information is given on any current masthead page.

Extended Molecular Mechanics Calculations of Thermodynamic Quantities, Structures, Vibrational Frequencies, and Infrared Absorption Intensities of Formic Acid Monomer and Dimer

Isao Yokoyama, Yoshihisa Miwa, and Katsunosuke Machida*

Contribution from the Faculty of Pharmaceutical Sciences, Kyoto University, Sakyo-ku, Yoshida, Kyoto 606, Japan. *Received January 22, 1991*

Abstract: The molecular mechanics simulation of infrared absorption spectra utilizing the effective atomic charges and charge fluxes as both the potential and the intensity parameters has been applied to formic acid monomer and dimer. The thermodynamic properties, optimized geometries, vibrational frequencies, and infrared absorption intensities are consistently derived from the potential models in which the difference between the monomer and the dimer is empirically taken into account. The large splitting between the A_g and the B_u cabonyl stretching frequencies of the dimer and the extension of the carbonyl bond on the dimerization are simultaneously reproduced by introducing two charge fluxes $\partial q_{O=C}/\partial r_{C=O}$ and $\partial q_{O-H}/\partial r_{C=O}$. The charge flux $\partial q_{OH}/\partial r_{OH}$ is responsible for the large frequency shift and intensification of the OH stretching band on the dimerization.

In our previous two reports,[1] an extended scheme of the molecular mechanics calculation was presented with illustrative simulations of vibrational spectra of *n*-alkanes and *n*-alkyl ethers. The empirical force field used in these works includes the Coulomb potential parameters in the form of effective charges of the atoms and their fluxes through the bonds on the change of bond lengths and valence angles (ECCF model[2]). The charge fluxes represent the deformability of the atomic charges during the nuclear motions.[2,3] These atomic charges and charge fluxes were used also as parameters for predicting the infrared absorption intensities. The enthalpies, entropies, and structures of *n*-alkanes and aliphatic ethers were successfully derived from this potential model.[1]

The present work has been undertaken to apply this method to formic acid monomer and dimer, which have been taken as suitable starting materials for dealing with the carboxyl group and hydrogen-bonded systems. Carboxylic acids are typical polar molecules, whose atomic charges and charge fluxes should play much more important roles in determining molecular structures and infrared absorption intensities than in the cases of *n*-alkanes and *n*-alkyl ethers. Formic acid is thus expected to afford severe criteria for testing whether any set of Coulomb potential parameters can elucidate the experimental data of these physical properties with reasonable accuracy. It is well known that carboxylic acid molecules are hydrogen-bonded pairwise to form cyclic centrosymmetric dimers. An estimation of the potential parameters and vibrational intensity parameters for such a system should be useful for further extension of our approach in molecular mechanics to compounds of biological interest.

Calculation

The potential model used in our approach[1] consists of six sums of terms each containing one or two variables. Each term in the

$$V = \sum_i D_i \exp\{-a_i(r_i - r_i^0)\}[\exp\{-a_i(r_i - r_i^0)\} - 2] + \sum_i \tfrac{1}{2}F_i(R_i - R_i^0)^2 + \sum_{i,j} F_{ij}(R_i - R_i^0)(R_j - R_j^0) + \sum_i \sum_n \tfrac{1}{2}V_{ni}\{1 - (-1)^n \cos n\tau_{ni}\} + \sum_{i,j} \tfrac{1}{2}V_{NB}(r_{ij}) + \sum_{i,j} \tfrac{1}{2}q_i q_j (1/\epsilon_{ij} r_{ij}) \quad (1)$$

first sum in eq 1 represents the Morse potential for the change of the bond length r_i. The parameters D_i were first taken as the standard bond energies calculated from the thermodynamic data in the literature,[4,5] and so adjusted as to fit the heat of formation

(1) (a) Machida, K.; Noma, H.; Miwa, Y. *Indian J. Pure Appl. Phys.* **1988**, *26*, 197. (b) Miwa, Y.; Machida, K. *J. Am. Chem. Soc.* **1988**, *110*, 5183. (c) Miwa, Y.; Machida, K. *Ibid.* **1989**, *111*, 7733.
(2) Decius, J. C. *J. Mol. Spectrosc.* **1975**, *57*, 348.
(3) Gussoni, M.; Castiglioni, C.; Zerbi, G. *J. Phys. Chem.* **1984**, *88*, 600.
(4) CODATA recommended key values for thermodynamics, 1977: *J. Chem. Thermodyn.* **1978**, *10*, 903.

0002-7863/91/1513-6458$02.50/0